EXPERIMENTAL STUDY ON THE MECHANICS OF REGULAR WAVES

De Serio F. and **Mossa M.**
Department of Civil and Environmental Engineering
Water Engineering Division; Polytechnic University of Bari
Via E. Orabona, 4 – 70125 Bari, Italy
Ph.: +39 080 596 3285/3286 – fax: +39 080 596 3414
email: f.deserio@poliba.it, mossa@poliba.it

Abstract: The analysis of velocity and turbulent and wave Reynolds shear stress distributions in a regular wave field on a sloping bottom is the aim of the present study, because of their influence on many coastal processes, such as undertow currents, sediment transport and action on maritime structures.
In literature some models of irrotational and non irrotational waves introduce a phase shift between horizontal and vertical velocity components, which is actually different from the value predicted by classical theories (Rivero and S.-Arcilla, 1995; Deigaard and Fredsøe, 1989). Consequently some papers evidence that the wave Reynolds shear stresses are not nil, providing some equations to predict them. As observed by You (1997) and Damiani et al. (1999), these different models do not always match regarding the trend and the sign of the wave Reynold shear stresses, and they definitively need a confirmation on the basis of laboratory tests. Therefore the experimental investigation of the present study is a contribution to the validation of the models present in literature.
The technique used to examine the measured time series of the velocity components allowed us to study also the turbulent Reynolds shear stresses, whose effects are more evident close to the breaking region.

Keywords: waves, shear stress, regular waves, turbulence.

1. INTRODUCTION

Wave dynamics aspects are fundamental for the study of the interaction between coastal currents and sediment transport, as shown by Rivero and S.-Arcilla (1995), Deigaard and Fredsøe (1989), Damiani and Mossa (1999). The results of their researches show that the classical theories of regular waves have a limited range of validity and applicability.
Particularly, focusing on the wave induced circulation, most models neglect in the momentum equation the contribution of the correlation of horizontal and vertical wave velocity components (i.e. the wave Reynolds shear stresses), by arguing that the two wave velocity components are $\pi/2$ out of phase.
The present study shows the experimental results of a research that is being carrying out in this field. The paper presents the analysis of three regular waves with different characteristics, generated in the wave flume of the Department of Civil and Environmental Engineering - Water Engineering Division of the Polytechnic University of Bari.

2. GOVERNING EQUATIONS

The problem is governed by the Navier-Stokes equations and for simplicity is confined to a 2D frame, in which the waves propagate along the x direction and the z axis is directed vertically upward from the free surface. Taking into account that any physical quantity can be split into the steady mean flow component (i.e. time-averaged component), the fluctuation component due to the statistical contribution of the wave and the fluctuation component of the turbulence (Ting and Kirby, 1996), the velocity component u_i (i=1,2) can be expressed as follows:

$$u_i(x_i,t) = \langle u_i \rangle (x_i,t) + u_i'(x_i,t) = U_i(x_i) + \tilde{u}_i(x_i,t) + u_i'(x_i,t) \tag{1}$$

where t is the time quantity, x_1 and x_2 are respectively the x and z Cartesian coordinates, the angular brackets < > are an operator to take an ensemble average, the tilde symbol indicates the fluctuations due to the wave statistical contribution (or oscillating components), the prime symbol indicates the turbulent fluctuations and the capital letters or the over-bar indicate the steady mean flow (time-averaged components).

In the present study, where regular waves are analyzed, ensemble-averaged velocities were obtained by phase-averaging the measured signals over a great number of cycles. Then, these values were averaged to yield the time-averaged velocities. Consequently, turbulent fluctuations were obtained as the difference between the original time series and the ensemble-averaged velocities. Using the Cartesian tensor notation, the ensemble-averaged motion equations of an incompressible fluid are:

$$\frac{\partial \langle u_i \rangle}{\partial t} + \frac{\partial \langle u_i \rangle \langle u_j \rangle}{\partial x_j} = \frac{1}{\rho} \frac{\partial}{\partial x_j} \left(\Sigma_{ij} - \rho \langle u'_i u'_j \rangle \right) \tag{2}$$

where

$$\Sigma_{ij} - \rho \langle u'_i u'_j \rangle = -\langle p \rangle \delta_{ij} + 2\mu S_{ij} - \rho \langle u'_i u'_j \rangle \ , \tag{3}$$

ρ is the water density, δ_{ij} is the Kronecker delta, p is the hydrodynamic pressure, μ is the dynamic viscosity and

$$S_{ij} = \frac{1}{2} \left(\frac{\partial \langle u_i \rangle}{\partial x_j} + \frac{\partial \langle u_j \rangle}{\partial x_i} \right). \tag{4}$$

The motion is periodic, so the average over the period T of equation (2) becomes

$$\frac{\partial \overline{\langle u_i \rangle \langle u_j \rangle}}{\partial x_j} = \frac{1}{\rho} \frac{\partial}{\partial x_j} \left(\overline{\Sigma_{ij}} - \rho \overline{\langle u'_i u'_j \rangle} \right). \tag{5}$$

Using equation (1) and the continuity equation

$$\frac{\partial U_i}{\partial x_i} = 0 \tag{6}$$

it is possible to rewrite equation (5) in the following way

$$\frac{\partial}{\partial x_j} \left(U_i U_j + \overline{\tilde{u}_i \tilde{u}_j} + \overline{u'_i u'_j} \right) = \frac{1}{\rho} \left(-\frac{\partial P}{\partial x_j} \delta_{ij} + \mu \frac{\partial^2 U_i}{\partial x_j \partial x_j} \right). \tag{7}$$

The cross products $\overline{\tilde{u}_i \tilde{u}_j}$ and $\overline{u'_i u'_j}$ appearing in equation (7) are, respectively, the wave Reynolds stresses and the turbulent Reynolds stresses, apart from the contribution of the water density ($-\rho$).

Rivero and S.-Arcilla (1995) derived theoretically the vertical distribution of the wave Reynolds shear stresses in the following cases: irrotational non dissipative flow on sloping bottom (observing that they are nil only in the case of irrotational non dissipative flow on horizontal bottom); irrotational dissipative flow; and non irrotational flow.

It is important to highlight that these theoretical results must be validated by experimental measurements, as remarked by the same authors and You (1997). The present study is a contribution to this aim.

3. EXPERIMENTS

The 45 m long and 1 m wide wave channel used to carry out the tests is located in the laboratory of the Department of Civil and Environmental Engineering - Water Engineering Division of the Polytechnic University of Bari (Italy). A sketch of the wave flume is shown in Fig. 1. In particular it allows to locate 100 measurement sections, numbered up to the wave maker (section 100), with a center to center distance equal to 0.44 m.

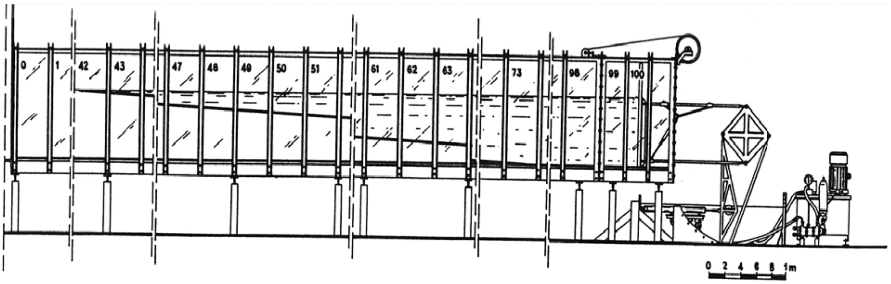

Fig. 1. Sketch of the wave flume.

From the wave paddle to section 73 the flume has a flat bottom, while from section 73 up to the shoreline it has a 1/20 sloped wooden bottom.

Table 1 shows the main characteristics of the tested regular waves, where d is the mean water depth, H and T the wave height and period, L_A the wave length according to the Airy theory, $U=HL_A{}^2/d^3$ the Ursell number and $\Pi=H/L_A[\coth(2\pi d/L_A)]^3$ the Goda parameter, indicators of a non linear wave behavior.

Taking into account the Irribarren breaking number ξ_b, the wave fields of the present study are characterized, respectively, by a spilling/plunging breaker in test 1 (ξ_b=0.37), a spilling breaker in test 2 (ξ_b=0.23), and a plunging breaker in test 3 (ξ_b=0.74).

The velocity field was measured using a backscatter, two-component, four beam LDA system and a Dantec LDA signal processor (58N40 FVA Enhanced) based on the covariance technique (Damiani and Mossa, 1999). The wave elevations were measured with a resistance probe placed in the transversal section of the channel crossing the laser measuring volume. The velocity and wave elevation measurements were assessed simultaneously, allowing us to perform the phase-averaging analysis. The velocity components measured in the present study are u in the x direction, conventionally established as positive if oriented onshore, and w in the vertical direction, conventionally established as positive if oriented upward. All the velocity measurements were assessed in many vertical sections between the bottom boundary layer and the wave trough.

4. DISCUSSION AND CONCLUSIONS

Figure 2 shows the vertical distributions along the channel of the time-averaged horizontal velocity components, for all the three tests. For each investigated section, the wave elevations $\tilde{\eta}$ are sketched above the $\overline{u}$ profile. From figure 2 it is possible to observe that for the most

measurement points the values are negative, i.e. offshore directed, while, confirming the mass continuity, they become positive, i.e. onshore directed, near the bottom (see sections 51 and 55 of test 2), and in the trough-crest region. As expected to be, the horizontal mean velocities are small in the offshore sections (section 63), where the wave behavior is similar to the linear one, while near the breaking region they increase, giving rise to the strong undertow current. Moreover it is possible to highlight that in all the tests the $\overline{u}$ vertical profiles show values close to zero near the bed with an increasing trend of their absolute values from the bottom to the free surface. The vertical profiles of figure 2 are quasi-triangular for tests 1 and 2, except for the breaking sections, while for test 3 they are quite flat along the vertical, due to the stronger turbulent effects typical of a plunging breaking.

	Section	*d [cm]*	*H [cm]*	*T [s]*	L_A *[m]*	*U*	*Π*	*Zone*
TEST 1 spilling/plunging	63	47.0	12.1	2.0	3.95	21	0.13	shoaling zone
	55	31.0	12.4	2.0	3.31	51	0.27	shoaling zone
	51	21.0	15.5	2.0	2.77	138	0.68	shoaling zone
	49	16.5	14.3	2.0	2.47	206	0.98	shoaling zone
	48	14.0	11.7	2.0	2.29	234	1.08	breaking zone
	47	11.3	5.9	2.0	2.06	181	0.82	breaking zone
	46	10.0	5.6	2.0	1.95	220	0.98	wave reforming
	45	8.5	4.9	2.0	1.80	266	1.17	wave reforming
	Section	*d [cm]*	*H [cm]*	*T [s]*	L_A *[m]*	*U*	*Π*	*Zone*
TEST 2 spilling	63	47.0	7.5	1.0	1.50	3	0.05	shoaling zone
	55	31.0	7.1	1.0	1.38	7	0.08	shoaling zone
	51	21.0	7.2	1.0	1.23	16	0.13	shoaling zone
	49	16.5	7.7	1.0	1.13	28	0.20	shoaling zone
	48	14.0	7.3	1.0	1.06	37	0.24	breaking zone
	47	11.3	7.1	1.0	0.97	55	0.33	breaking zone
	46	10.0	5.1	1.0	0.92	50	0.29	wave reforming
	45	8.5	4.6	1.0	0.86	62	0.35	wave reforming
	Section	*d [cm]*	*H [cm]*	*T [s]*	L_A *[m]*	*U*	*Π*	*Zone*
TEST 3 plunging	63	47.0	6.7	4.0	8.42	48	0.22	shoaling zone
	55	31.0	8.1	4.0	6.88	132	0.58	shoaling zone
	51	21.0	10.6	4.0	5.69	377	1.60	shoaling zone
	49	16.5	11.2	4.0	5.05	646	2.72	shoaling zone
	48	14.0	12.9	4.0	4.66	1033	4.32	near breaking zone
	48'	13.0	11.5	4.0	4.49	1068	4.45	breaking zone
	47	11.3	9.2	4.0	4.19	1131	4.70	breaking zone
	46	10.0	7.2	4.0	3.95	1130	4.68	wave reforming
	45	8.5	5.8	4.0	3.64	1260	5.20	wave reforming

Tab. 1. Main characteristics of the regular waves.

The mean values of the vertical velocity components, generally smaller than those of the horizontal ones, are not shown in the present paper for the sake of brevity.

The experimental data highlight a phase shift between $\widetilde{u}$ and $\widetilde{w}$ different from $\pi/2$ at each investigated depth, confirming the observations of Gudmestad and Connor (1980) and Rivero and S.-Arcilla (1995).

Figure 3 shows the vertical distributions of the correlations $\overline{\widetilde{u}\widetilde{w}}$ (i.e. wave Reynolds shear stresses, apart from the water density -ρ) for all the measurement points. Again, the phase-averaged wave surface profiles are sketched above each section.

For all the tests, it is evident that in the sections offshore the breaking region, the vertical trend of $\overline{\tilde{u}\tilde{w}}$ is quite linear, generally decreasing with the distance from the bottom. Taking into account the convention of the velocity signs, the maximum positive values are located near the bed; on the contrary, negative values are present in the points closer to the wave trough. In particular, in the section 63 the trend of $\overline{\tilde{u}\tilde{w}}$ is quasi bi-triangular. These results are in agreement with those of Rivero and S.-Arcilla (1995; 1997); in fact both the sign (positive) and the trend (decreasing upwards) of the vertical distribution of $\overline{\tilde{u}\tilde{w}}$ is correctly predicted by the model of the authors. Approaching the breaking region (sections 49 and 48 of test 1 and test 2, and sections 49, 48 and 48' of test 3) it is possible to observe that $\overline{\tilde{u}\tilde{w}}$ are always positive. Also the aforementioned results agree with the theoretical distributions proposed by Rivero and S.-Arcilla (1995) for the case of dissipative waves propagating over a sloping bottom. The theoretical model for dissipative waves over a sloping bottom proposed by Deigaard and Fredsøe (1989) seems to be validated by $\overline{\tilde{u}\tilde{w}}$ trends in the breaking zone and also in the wave reforming zone, where the vertical profile has an increasing trend from the bottom up to the free surface (see sections 47, 46 and 45 of test 1, sections 47 and 46 of test 2 and sections 47 and 46 of test 3).

Figure 4 shows the vertical distributions of the turbulent velocity cross correlations $\overline{u'w'}$ (i.e. turbulent Reynolds shear stresses, apart from the water density -ρ). A comparison with the wave Reynolds shear stresses highlight that $\overline{u'w'}$ are generally smaller. Moreover in the sections far from the breaking region, the values of $\overline{u'w'}$ are always quite nil. They become greater only where the turbulence is not too weak, that is only close to the breaking zone and wave reforming zone, showing a triangular trend with negative values for the most measurement points.

REFERENCES

Damiani L., Mossa M. (1999), O*n turbulence in a wave field*, Proc. of COPEDEC, Cape Town, South Africa, vol.1, pp.25-36.

Damiani L., Mossa M., Arcilla A.S. (1999), *Vertical distribution of the wave Reynolds shear stresses in a regular wave field,* Giornate di Studio sulla "Difesa Idraulica del Territorio", Trieste, pp.425-474.

Deigaard R., Fredsøe J. (1989), *Shear stress distribution in dissipative water waves,* Coastal Engineering 13, pp.357-378.

Gudmestad O.T., Connor J.J. (1980), *Engineering approximation to non linear deep water waves,* Journal of Applied Ocean Research, 8, pp.76-88.

Rivero F.J., Arcilla A.S. (1995), *On vertical distribution of* $\langle\overline{\tilde{u}\tilde{w}}\rangle$, Costal Engineering 25, pp.137-152.

Rivero F.J., Arcilla A.S. (1997), *Discussion on the vertical distribution of* $\langle\overline{\tilde{u}\tilde{w}}\rangle$*: reply to the comments of Z.J. You,* Coastal Engineering 30, pp.311-315.

Ting F.C.K., Kirby J.T. (1996), *Dynamics of surf-zone turbulence in a spilling breaker,* Coastal Engineering 27, pp.305-310.

You Z.J. (1997) *Discussion on the vertical distribution of* $\langle\overline{\tilde{u}\tilde{w}}\rangle$ *by F.J. Rivero and A.S. - Arcilla: comments,* Coastal Engineering 30, pp.305-310.

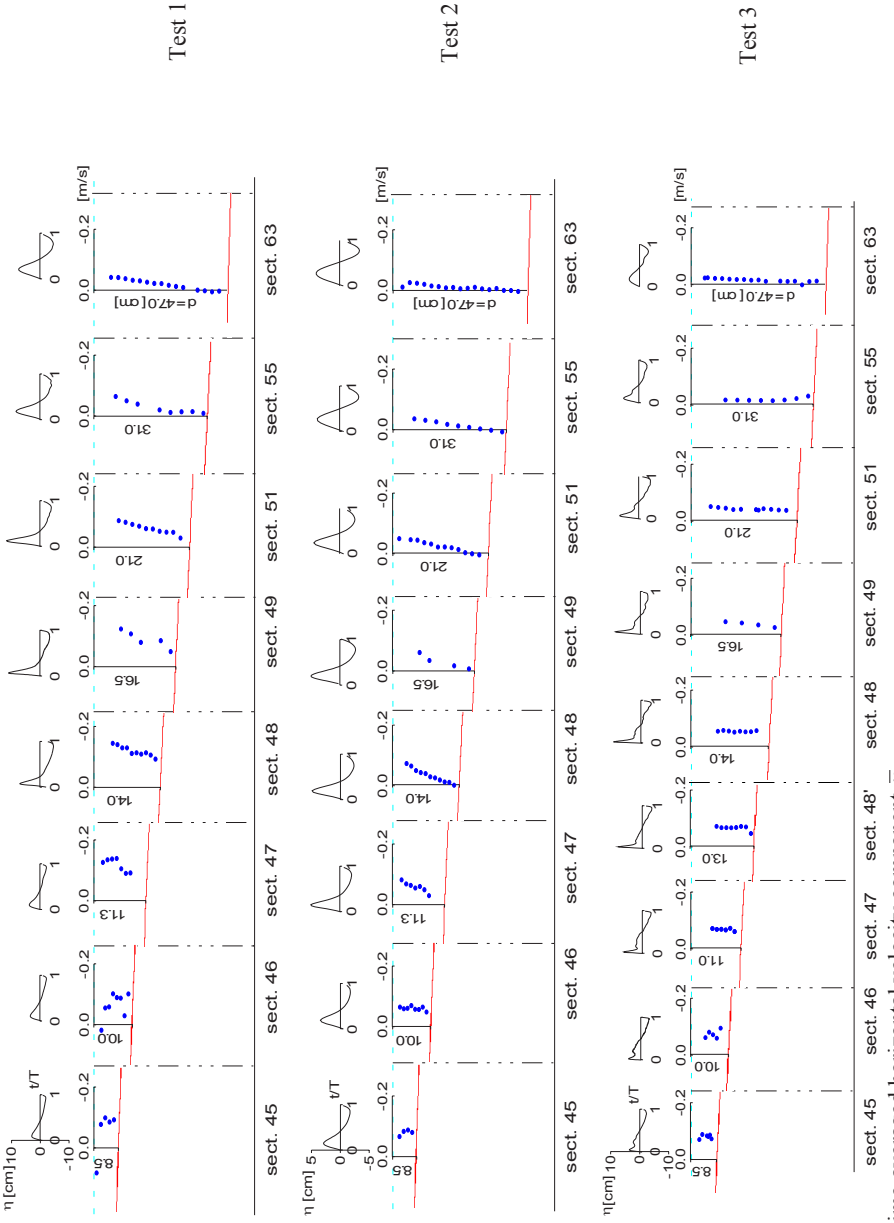

Fig. 2. Time-averaged horizontal velocity component $\overline{u}$.

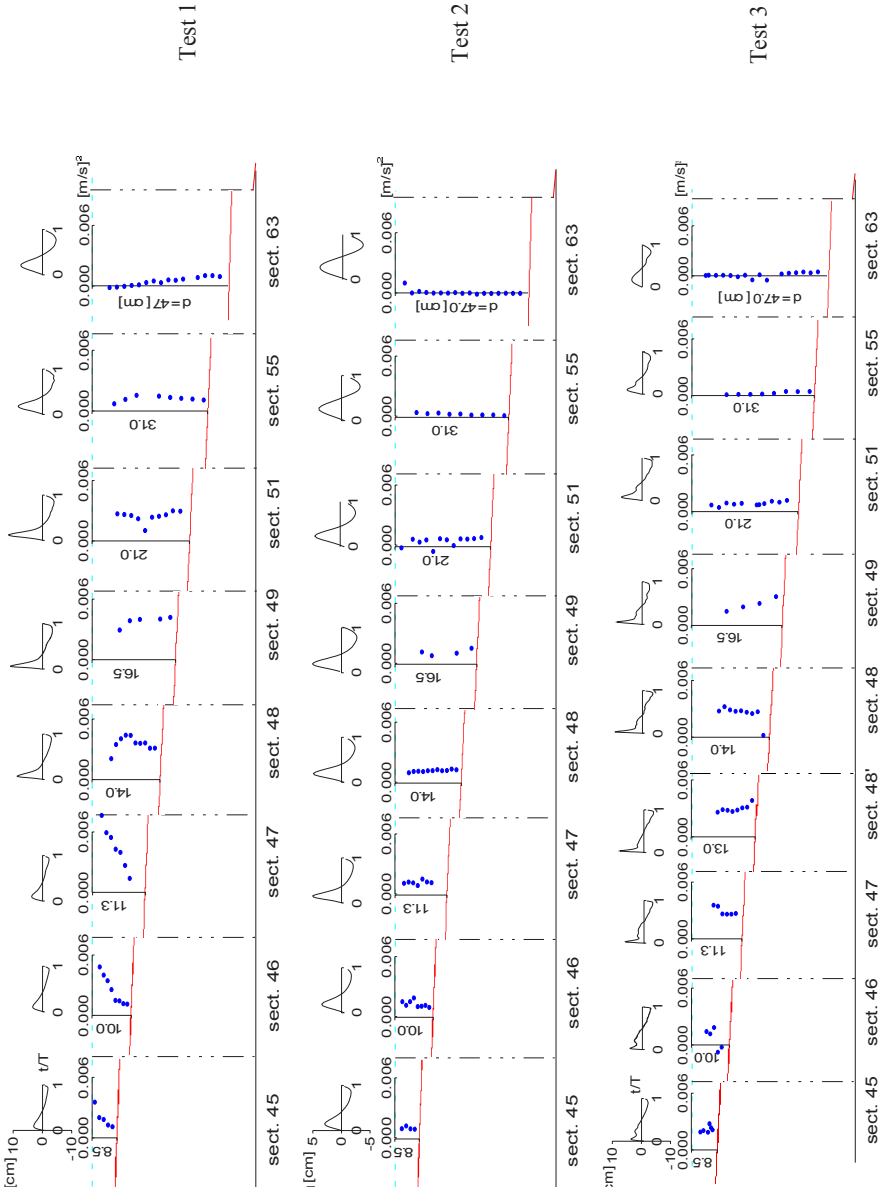

Fig. 3. Vertical distribution of the correlations $\widetilde{u}\widetilde{w}$.

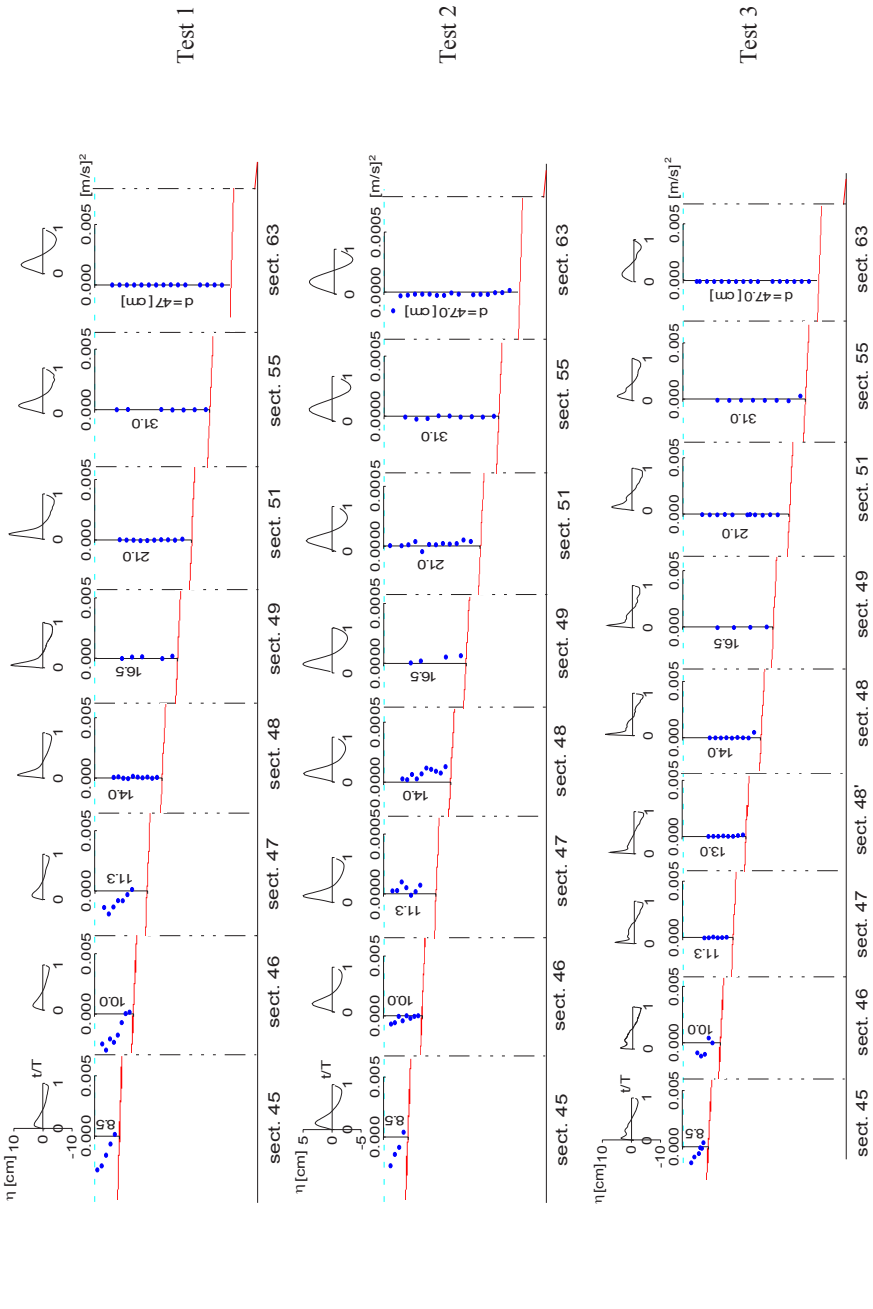

Fig. 4. Vertical distribution of the correlations $\overline{u'w'}$.